

Universiteit Leiden



The handle http://hdl.handle.net/1887/25721 holds various files of this Leiden University dissertation.

Author: Klooster, Ronald van 't

Title: Automated image segmentation and registration of vessel wall MRI for quantitative

assessment of carotid artery vessel wall dimensions and plaque composition

Issue Date: 2014-05-07

Chapter 2

Automatic lumen and outer wall segmentation of the carotid artery using deformable 3D models in MR angiography and vessel wall images

This chapter was published in:

R. van 't Klooster, P. J. H. de Koning, R. A. Dehnavi, J. T. Tamsma, A. de Roos, J. H. C. Reiber, R. J. van der Geest. Automatic lumen and outer wall segmentation of the carotid artery using deformable three-dimensional models in MR angiography and vessel wall images, *Journal of Magnetic Resonance Imaging*, Volume 35, Issue 1, Pages 156–65, 2012.

Abstract

Purpose: To develop and validate an automated segmentation technique for the detection of the lumen and outer wall boundaries in MR vessel wall studies of the common carotid artery.

Materials and methods: A new segmentation method was developed using a three-dimensional (3D) deformable vessel model requiring only one single user interaction by combining 3D MR angiography (MRA) and 2D vessel wall images. This vessel model is a 3D cylindrical Non-Uniform Rational B-Spline (NURBS) surface which can be deformed to fit the underlying image data. Image data of 45 subjects was used to validate the method by comparing manual and automatic segmentations. Vessel wall thickness and volume measurements obtained by both methods were compared.

Results: Substantial agreement was observed between manual and automatic segmentation; over 85% of the vessel wall contours were segmented successfully. The interclass correlation was 0.690 for the vessel wall thickness and 0.793 for the vessel wall volume. Compared with manual image analysis, the automated method demonstrated improved interobserver agreement and inter-scan reproducibility. Additionally, the proposed automated image analysis approach was substantially faster.

Conclusion: This new automated method can reduce analysis time and enhance reproducibility of the quantification of vessel wall dimensions in clinical studies.

2.1. Introduction

2.1 Introduction

Atherosclerosis is a progressive disease which, at an early stage, is characterized by vessel wall thickening causing outward remodeling, then narrowing of the lumen, and at a later stage by the formation of plaque lesions inside the vessel wall [3]. In patients with unstable plaques, the thin fibrous cap can rupture causing the plaque contents to enter the vessel lumen causing a stroke. Therefore, accurate assessment of the vessel wall dimensions and composition of the vessel wall is essential for identifying patients at risk. The 3.0 Tesla (T) MRI offers high-resolution noninvasive imaging of the vessel wall of the carotid artery. For quantitative assessment of the vessel wall morphology and plaque composition, contours describing the boundaries of the vessel wall are needed [38]. Vessel wall thickness measurements have been shown to correlate well with ultrasound (US) intima media thickness measurements (IMT) [33, 44, 45]. IMT has emerged as a marker for cardiovascular disease and has been used as an endpoint in clinical trials assessing the effect of pharmacological treatment of systemic atherosclerosis [46,47]. In turn, MRI is also used in clinical trials [48,49], but compared with US, it offers the advantage that it can provide a 3D image of the vascular structure instead of a 2D image that is dependent on the angle of insonation [45]. Other advantages of MRI over US are lower measurement variability [45], enabling smaller sample sizes and potentially shorter study duration in clinical trials.

Currently, quantitative assessment of the vessel wall dimensions is based on manual tracing of the lumen and outer wall boundaries, which is timeconsuming and subject to inter- and intra-observer variation. Consequently, computerized segmentation techniques have been developed to overcome these limitations. Reported methods range from interactively guiding a segmentation algorithm [31, 32] to approaches requiring one user interaction per imaging section [25] or one interaction to start the complete segmentation process [33, 34]. Despite the advances in automated vessel wall contour detection techniques, further improvements are needed to improve the accuracy, robustness and speed of automated quantitative vessel wall analysis. Further improvements might be accomplished by applying 3D registration and segmentation techniques, instead of 2D methods that process each slice independently of all other slices.

Accordingly, the purpose of this study was to develop a highly automated 3D image segmentation technique for the detection of the lumen and outer wall boundaries in MR vessel wall imaging studies of the common carotid artery.

We present an automatic segmentation method that uses combined Time of Flight (TOF) MRA and vessel wall images to segment the vessel wall using deformable 3D tube models. The combination of the two types of images potentially decreases user interaction, and increases segmentation performance. By using a 3D approach, the image segmentation can take advantage of information in neighboring slices in case there is little image information in a slice, and in case of isotropic 3D datasets, the method can gain full advantage of the extra available image information. The performance of this new method is evaluated by comparing the automatic segmentations with manual segmentations of carotid vessel wall imaging studies of 45 subjects. In addition, inter-observer variability, as well as inter-examination reproducibility were investigated for both manual and automated assessment of vessel wall parameters.

2.2 Materials and methods

Subjects

Forty-five adult subjects (56% male; 19-79 years old; mean age = 52 years) underwent a carotid MRI on a 3T scanner (Achieva; Philips, Best, The Netherlands). A variation of cardiovascular risks was present in the group, but none of the subjects had symptoms of cardiovascular disease. Ten subjects, randomly chosen from the group of 45 subjects, were imaged twice, at baseline (T_0) and at a maximum of 28 days later (T_1), resulting in a total of 55 MR studies. The subjects were imaged in the supine position with the neck positioned at the isocenter of the magnet. In all subjects the left carotid artery was examined.

MR image acquisition

A scan protocol was applied, which was tailored to obtain a series of oblique axial slices perpendicular to the course of the left common carotid artery starting at the level of the flow divider and ending in the common carotid artery, as previously described by Alizadeh Dehnavi et al [50]. Automated vessel wall contour detection was based on processing of the TOF-MRA survey scan and high resolution vessel wall images. The TOF-MRA was acquired with the following parameters: 20 contiguous transversal slices, fast gradient-echo sequence, acquired pixel size = 1 mm x 1.23 mm x 5.0 mm, field of view (FOV) = 300 mm, echo time (TE) = 3.8 ms, repetition time (TR) = 7.7 ms, and flip angle = 20° . The parameters for the vessel wall images, a black-blood sequence, were: an electrocardiograph triggered dual IR spoiled segmented k-space FGRE sequence, 8 slices, no slice gap, acquired pixel size = 0.46 mm x 0.46 mm x 0.46 mm x 0.46 mm, reconstructed pixel size = 0.27 mm x 0.27 mm x 0.27 mm x 0.27 mm, FOV = 0.46 mm, TE = 0.46 ms, TR = 0.46 m

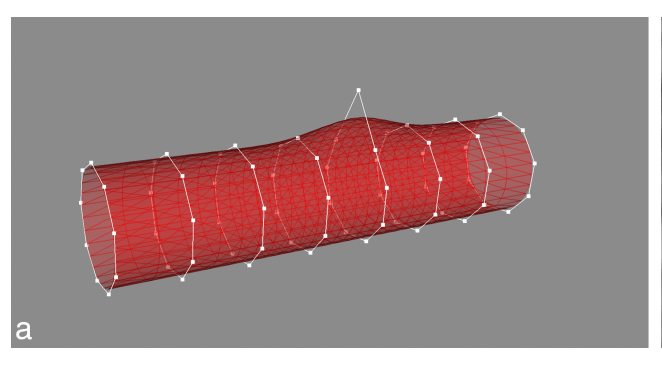
Automatic image segmentation

The automated segmentation algorithm is initialized by specifying the artery of interest in the MRA image of the neck area. This image provides a global overview of the arterial structure and allows users to easily identify the artery segment by manually indicating a proximal and a distal point in one of the image slices or on the maximum intensity projection of the 3D volume. Based on these two points, the following five steps are performed automatically, resulting in a segmented vessel wall in the vessel wall images: (1) Detection of the arterial lumen in the MRA image; (2) Transfer and registration of the MRA lumen segmentation to the vessel wall images; (3) Refinement of the lumen boundary in the vessel wall images; (4) Estimation of initial outer wall boundary; (5) Detection of the outer wall boundary in the vessel wall images.

In steps 1, 3, and 5, a segmentation algorithm based on the fitting of a 3D cylindrical NURBS surface is used.

3D Cylindrical NURBS surface segmentation applied to carotid arteries

A 3D Cylindrical NURBS surface is used to model the anatomy of vascular structures [51, 52] (Fig. 2.1). This model possesses several advantageous properties, such as local control of shape and the flexibility to describe both simple and complex objects. The surface is



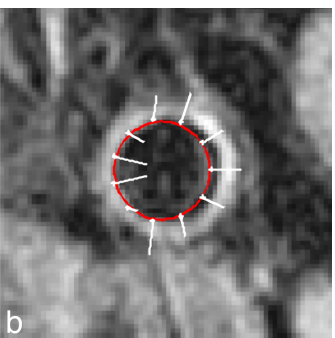


Figure 2.1: a) Cylindrical NURBS surface (red tube) with local change in shape enforced by two control points (white points, the control points are connected by straight lines for illustrative purpose). b) The 2D vessel wall image example showing image forces (white lines) acting on the control points (white points) and the corresponding lumen contour (red).

defined by several spatially distributed control points. Increasing the number of control points allows the creation of more complex surfaces. By moving the control points (see Fig. 2.1b), the surface can by relocated. For this application, the surface is relocated to fit the underlying image data by iteratively moving the control points such that the surface is moved toward edges in the image.

In this study, a tube model is initialized by creating multiple rings with control points positioned perpendicular to the detected vessel axis. For each ring, the diameter and number of control points must be specified. The fitting of the surface to the image data is performed by iteratively moving the control points. The movement of a control point is derived from image forces acting on nearby surface points. The closer the surface point is to the control point, the more influence it has on the control point. In each iteration, an image force is calculated at each surface point. This image force is the desired movement to move the surface point to the structure of interest, for example, an edge, in the image. The image force at each surface point is calculated as follows and is illustrated in Figure 2.2: (i) A signal intensity (SI) profile along the surface normal, centered at the surface point is obtained. The SI values are obtained by 3D linear interpolation of the image information. (ii) The SI profile is analyzed by detecting the strongest edge in a particular direction. The direction can either be positive, from low to high SI values, or negative, from high to low SI values. If the direction is not set, the strongest edge is selected. (iii) The image force vector for that surface point is then proportional to the distance of the strongest edge with respect to the center of the SI profile multiplied by the surface normal.

The exact influence of the surface points on a control point can be calculated analytically from the description of the NURBS surfaces [53]. The closer the surface point is located to a control point, the more influence it has on the control point. At the end of each iteration, the image forces acting on the surface points are applied to the control points. Finally the position of the control points in each ring is constrained in such a way that the ordering of the points remains unchanged and a minimum distance between control points is enforced. The fitting algorithm can be adapted to a specific situation by changing the width of the SI profile and by selecting a positive or negative edge direction. The SI profile width represents the search range for edges in the image. If the initial tube

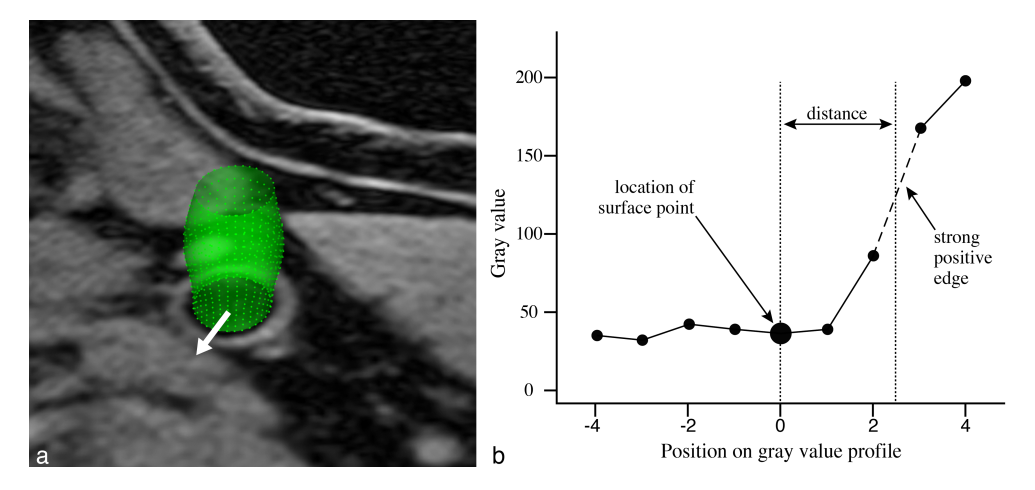


Figure 2.2: a) Intermediate result of fitting the lumen tube. The green points are the surface points, the white arrow shows the signal intensity (SI) profile along the surface normal. b) SI profile corresponding to the white arrow and detection of the strongest positive edge.

surface is expected to be far from the final segmentation, a large SI profile width has to be chosen.

Detection of the arterial lumen in the MRA image

The automatic image segmentation is initialized by the manual selected proximal and distal point specifying the artery segment of interest. Subsequently, a 3D curve inside the arterial lumen and an estimation of the lumen diameter between the indicated points is found using Wavefront propagation based on fast marching level sets [51, 54, 55]. A tube model is initialized by generating rings with control points perpendicular to the curve and fitted to the image data. Each ring was centered on the curve and the diameter was set to the estimated lumen diameter obtained before. During the fitting, the control points were allowed to move in 3D space, the width of the SI profile was set to 2 mm, the number of iterations was 50 and the surface was fitted to edges in the image which are bright inside the vessel model and dark outside.

Transfer and registration of the MRA lumen segmentation to the vessel wall images

The 3D MRA lumen segmentation is transferred to the 2D vessel wall slices by intersecting the tube model with the vessel wall slices based on their known geometrical relation. Subsequently, a 2D lumen contour is extracted for each vessel wall slice. Direct transfer of the tube model to the vessel wall images is not possible because the locations of the control points do not correspond with the 2D slices. Also, the higher resolution of the vessel wall images requires the usage of more control points to accurately describe the lumen boundary. To compensate for possible patient motion during the scanning of the different sequences, an automatic registration step is applied before the transfer of the MRA lumen segmentation to ensure that the extracted lumen contours are correctly aligned to the lumen boundaries in the vessel wall images.

The automatic registration is based on the assumption that the lumen boundary is a dominant circular structure in the vessel wall image near the transferred MRA lumen contour. A Hough transform, which is an image processing algorithm that can be used to detect circular structures, was applied to the vessel wall images to generate an image that has high signal intensities at the center of circular structures. Subsequently, the 3D MRA lumen tube was translated and rotated to include the highest responses from the Hough transform inside the tube. Least squares optimization was used to find the best fit resulting in a 3D tube which is registered to the vessel wall images. In case this registration step was deemed unsuccessful, the user was able to correct the registration.

Refinement of the lumen boundary in the vessel wall images

The set of registered lumen contours was used to initialize a new tube model in the vessel wall images. In each vessel wall slice, a ring with control points was created by placing the control points equidistantly on the registered contour. The tube model is fitted to the image data with the constraint that the control points were only allowed to move within the image slice. The width of the SI profile was set to 2 mm, the number of iterations was 50 and the surface was fitted to edges in the image which are dark inside the vessel model and bright outside. The result of this step is the lumen tube.

Estimation of the initial outer wall boundary

The lumen tube is intersected by the vessel wall slices and for each slice a 2D contour is extracted. An estimate of the outer wall boundary is found by dilating these contours from 0.5 to 2.0 mm in steps of 0.05 mm. For each step, the average edge strength under the contour was calculated, taken into account an edge direction from bright to dark. The dilated contour with the strongest average edge strength was selected as the initial outer wall boundary for that slice. This process was repeated for every slice resulting in an estimation of the outer wall boundary.

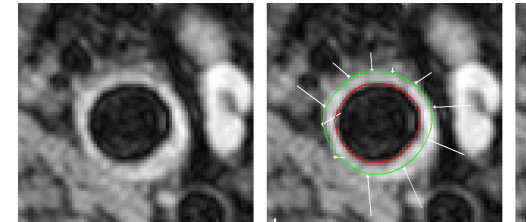
Detection of the outer wall boundary in the vessel wall images

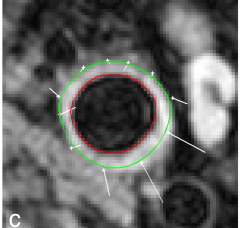
The outer wall is detected in a similar manner as was done for the lumen boundary. Because the initial outer wall boundary is estimated at the position of the expected outer boundary, the SI profile width was limited to 1 mm. The tube surface is fitted to edges in the image which are bright inside the vessel model and dark outside. An example of the fitting of the outer tube is given in Figure 2.3.

The final segmentation of the vessel wall is defined by the lumen tube and the outer tube and is used to derive various quantitative carotid vessel wall parameters, described below.

Manual image analysis

All images were manually analyzed using the VesselMASS software package [25], by an experienced radiologist (M_1) . Ten scans, the T_0 group, were analyzed by a second radiologist (M_2) . Each observer independently traced the lumen and outer wall boundaries of the vessel wall in the axial slices of the black-blood sequence. The obtained contours from observer M_1 were used as the gold standard.





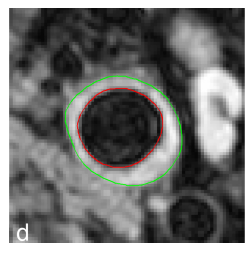


Figure 2.3: Model fitting process for the outer vessel wall shown in 2D. a) T1W image slice. b) First iteration showing the image forces that act on the control points (white). c) Intermediate result. d) The final result after 50 iterations.

Automatic image analysis procedure

The same set of images was analyzed with the automatic image segmentation method. To study the effect of initialization on the segmentation result, two users (A_1 and A_2) independently analyzed the T_0 subset of 10 carotid arteries with the automatic image segmentation algorithm. The automatic image segmentation method was implemented in C++ and all analyses were performed on a standard PC with a quad-core processor running at 2.4 GHz (Intel Q6600) and 4 GB of RAM. For both the manual and automatic image analysis, the duration of the analysis was recorded.

Definition of quantitative parameters

Vessel wall thickness and volume measurements

The vessel wall thickness (VWT) was derived automatically by first determining the centerline between the lumen and outer contour in each vessel wall slice. Then 100 chords connecting the lumen and outer wall contour were equidistantly sampled perpendicular to that centerline. For each slice, the median of the length of these 100 chords was calculated, and the average of the measurements of all slices resulted in the VWT. The user was able to visualize the individual VWT measurement chords in 3D by color mapping the VWT on the segmentation of the lumen (Fig. 2.4) enhancing visual inspection of the vessel structure. The vessel wall volume (VWV) was calculated by summing the vessel wall area in each slice and then multiplying that sum by the slice thickness.

Contour comparison metric

To compare the performance of the automatic segmentations with the reference standard in more detail, the degree of similarity (DoS) was calculated for the contours in each analyzed image slice [56]. The DoS is defined as the percentage of points that is similar between two contours. The number of sample points per contour was 100, obtained by equidistant sampling. Pairs of corresponding points are assumed to be similar if the distance between two points does not exceed a certain threshold. The threshold was chosen to be 0.27 mm, which is similar to the reconstructed pixel size (0.27 x 0.27 mm). An example is given in Figure 2.5. Similar points are interpreted as successfully segmented, while dissimilar points need adjustments to match the expert segmentation. The DoS allows evaluating the lumen and outer contours independent of each other.

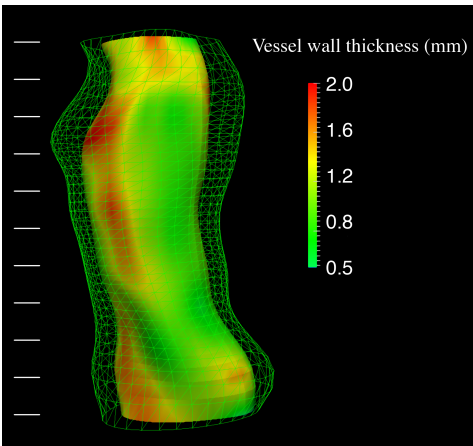


Figure 2.4: Final vessel wall segmentation showing the lumen with the vessel wall thickness color-coded on it, the outer wall (green wireframe) and slice levels (white lines).

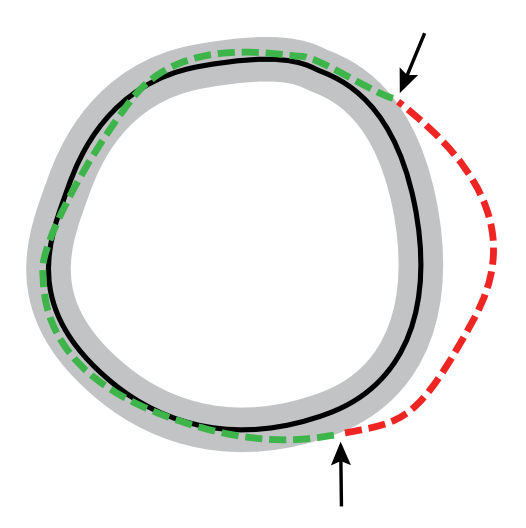


Figure 2.5: Example of a degree of similarity of 73%. The solid line is the reference contour; the grey band shows the 0.27 mm margin. The dashed line represents the computed contour. A total of 73% of the solid line coincides with the dashed line

Comparison and statistical analysis

Automatic versus manual segmentation

The performance of the automatic segmentation method was quantified by calculating the DoS between the automatic segmented and manual contours. The agreement between both methods was evaluated by calculating the mean, standard deviation and intraclass correlations including 95% confidence intervals for the VWT and VWV found by manual and automatic segmentation. A paired t-test was performed to assess whether the means of both methods differed. Bland-Altman plots [57] for both parameters were generated to investigate the limits of agreement between automated and manual analysis. A P-value smaller than 0.05 was considered significant.

Interobserver agreement and reproducibility

To estimate the interobserver agreement, ten subjects were analyzed twice, each time by a different observer; this was done for both the manual segmentation as well as the automatic segmentation method. Bar plots were used to evaluate the variability between different observers and also the DoS was determined. To assess reproducibility, intraclass correlations including 95% confidence intervals between the time points T_0 and T_1 were determined for the VWT and VWV.

Table 2.1: Comparison between the automatic and manual segmentation using one manual and one automatic observer.

	Manual vs. automatic $[n = 45]$		
	Mean of differences ± SD	ICC [CI]	
VWT (mm)	$0.12 \pm 0.21 \ (P < 0.01)$	0.690 [0.500-0.817]	
VWV (mm ³)	$45.39 \pm 80.16 \ (P < 0.01)$	0.793 [0.682-0.892]	

VWT = vessel wall thickness; VWV = vessel wall volume; SD = standard deviation; *P*, P value of t-test; ICC = intraclass correlation; CI = confidence interval.

Table 2.2: Interobserver analysis using two manual and two automatic observers.

	Inter-observer analysis $[n = 10]$				
	M ₁ vs. M ₂		A ₁ vs. A ₂		
	Mean of differences ± SD	ICC [CI]	Mean of differences ± SD	ICC [CI]	
VWT (mm)	$-0.04 \pm 0.05 \ (P = 0.02)$	0.975 [0.904-0.994]	$0.01 \pm 0.03 \ (P = 0.24)$	0.986 [0.945-0.997]	
VWV (mm ³)	$-7.51 \pm 18.69 (P = 0.41)$	0.985 [0.942-0.996]	$0.95 \pm 4.61 \ (P = 0.53)$	0.999 [0.996-0.998]	

VWT = vessel wall thickness; VWV = vessel wall volume; SD = standard deviation; *P*, P value of t-test; ICC = intraclass correlation; CI = confidence interval.

2.3 Results

Automated versus manual segmentation

The time needed to automatically segment the TOF-MRA and vessel wall images of one subject was approximately 18 s after indicating the artery of interest. Indication of the artery of interest was completed within 30 s by the user. A manual analysis took on average 12 min including visual identification of the artery of interest. The average DoS for 45 studies was $96.2\%~(\pm~5.4\%)$ for the lumen contour and $75.3\%~(\pm~17.7\%)$ for the outer contour, which is an average of 85.7% for both contours. The DoS values indicate better performance of the automatic segmentation for the lumen than for the outer contour. The systematic error, standard deviations, P-value of the paired t-test and intraclass correlations, including 95% confidence intervals, for the quantitative measurements are given in Table 2.1. The automatic segmentation algorithm shows substantial agreement [58] for both the quantification of VWT and VWV.

Bland-Altman analysis for the quantitative parameters is given in Figure 2.6. The figures show a small but significant underestimation, as indicated by the paired t-test, of the VWT and VWV of respectively 10.5% and 11.9% by the automatic segmentation method. A significant upward trend is observed for the VWT (r = 0.65; P < 0.001) and VWV (r = 0.67; P < 0.001).

Interobserver agreement and reproducibility

Bias of the mean, standard deviations of the difference, and intraclass correlations between the two pairs of observers (M_1 and M_2 , A_1 and A_2) and the multiple time points (T_0 , T_1) are given in Tables 2.2 and 2.3.

The intraclass correlations between different observers show that the analysis reproducibility of the automated segmentation method is higher than the manual segmentation. The DoS of the lumen and outer contour for manual experts was 97.8% and 92.3%, these numbers were higher for the automatic observers (A_1 and A_2); 99.8% for the lumen

2.4. Discussion 23

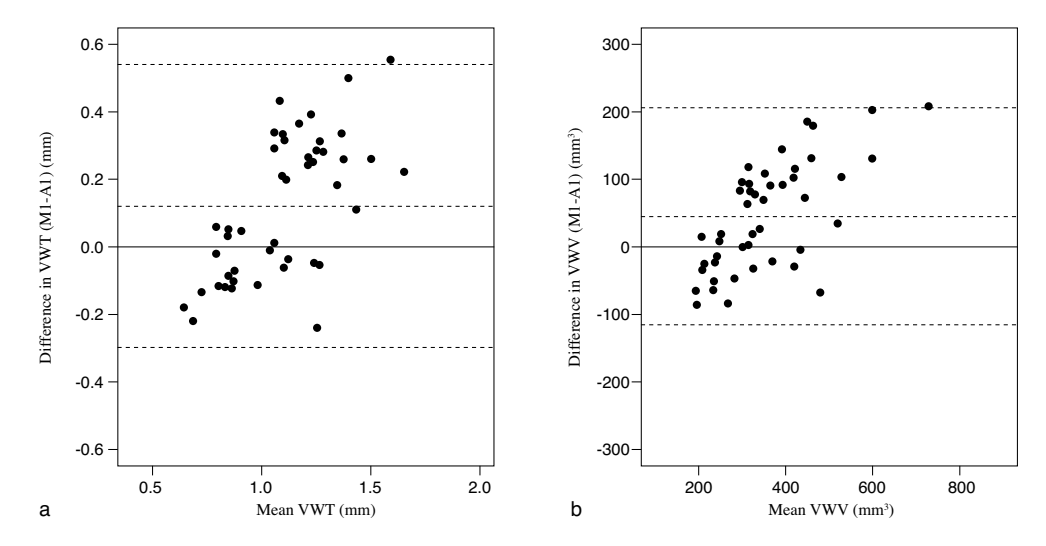


Figure 2.6: Bland-Altman plots showing the comparison between the manual and automatic segmentation for (a) vessel wall thickness (VWT) and (b) vessel wall volume (VWV).

Table 2.3: Scan-rescan analysis using one manual and one automatic observer.

	Scan-rescan analysis $[n = 10]$				
	T ₀ vs. T ₁ (M ₁)		T ₀ vs. T ₁ (A ₁)		
	Mean of differences ± SD	ICC [CI]	Mean of differences ± SD	ICC [CI]	
VWT (mm)	$-0.06 \pm 0.11 \ (P = 0.13)$	0.830 [0.457-0.955]	$-0.02 \pm 0.06 \ (P = 0.12)$	0.940 [0.780-0.985]	
VWV (mm ³)	$-12.82 \pm 24.62 \ (P=0.44)$	0.976 [0.908-0.994]	$-3.62 \pm 21.10 \ (P = 0.60)$	0.983 [0.934-0.996]	

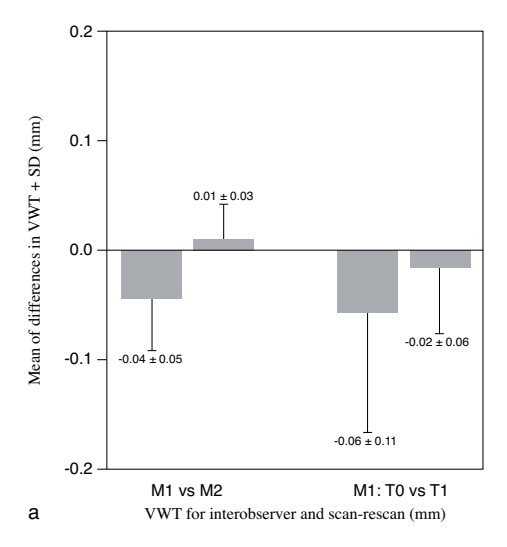
VWT = vessel wall thickness; VWV = vessel wall volume; SD = standard deviation; *P*, P value of t-test; ICC = intraclass correlation; CI = confidence interval.

contour and 99.0% for the outer contour. No significant bias was found in both clinical measures for the automated method, contrary to the VWT as measured by the manual observers (Table 2.2). Figure 2.7 shows a smaller bias and variation of the VWT and VWV measurement with the automatic segmentation method. These results indicate a lower interobserver variability when compared with the manual segmentation method.

Finally, inter-scan reproducibility was assessed by correlating the clinical measurements found on T_0 and T_1 (see Table 2.2). The intraclass correlations for both metrics were higher for the automated segmentation method. Figure 2.7 shows a smaller bias and variation for the automatic segmentation method indicating better reproducibility of the automatic method.

2.4 Discussion

In this study, a 3D method was presented for automated segmentation of the vessel wall of the common carotid artery in combined MRA and vessel wall images. To our knowledge this is the first approach using a true 3D model which can be applied to both isotropic and nonisotropic image data. Comparison of the automated method with manual segmentation shows substantial agreement, with slight underestimation and a proportional error of the vessel wall thickness and volume. Compared with manual image analysis,



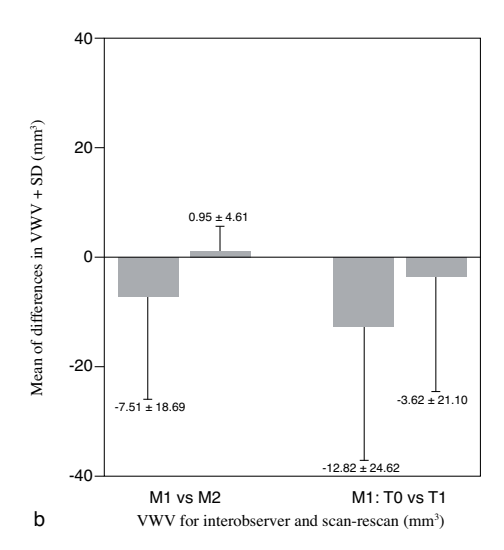


Figure 2.7: Bar plots showing interobserver variation and intra-scan reproducibility of (a) vessel wall thickness (VWT), (b) vessel wall volume (VWV).

the automated method demonstrated improved interobserver agreement and inter-scan reproducibility. Additionally, the proposed automated image analysis approach was substantially faster.

The performance of the automatic segmentation method is similar to existing methods which are all based on a 2D approach. In line with previous research, automated segmentation of outer contours was shown to be more difficult than lumen contours. Based on visual inspection, Underhill et al [33] report that 100% and 93% of the lumen and outer contours were successfully segmented, respectively. However, the detected contours were not compared with an independent manual reference. In our study, we used the DoS to compare the automated segmentation results with the manual reference. Using this stricter metric, 96.2% of the lumen contour was successfully segmented while this was 75.3% for the outer contour. The results of our repeatability study show a smaller variability for measurement of the VWT compared with the method developed by Underhill et al.

Adame et al [25] presented a different automated analysis approach, which requires one user interaction per slice. First, the outer wall is detected by fitting an ellipse to the image data, and then the lumen contour is found by clustering. Comparison of our results with this method is not straightforward, because different quantitative measures are used and our scores are based on a subject level and not on a slice level. However, our method requires less user interaction and the shape of the outer contour is not constrained to an ellipse.

In a more recent study [34], it was shown that a decrease in user interaction and an increase in segmentation performance can be accomplished by combining the MRA and VWI images. Our method uses a similar workflow but the registration and segmentation methods are 3D, instead of 2D.

Although image quality varied between and within subjects (Figs, 2.8,2.9,2.10), no images were excluded from the evaluation and no manual corrections were applied to any

2.4. Discussion 25

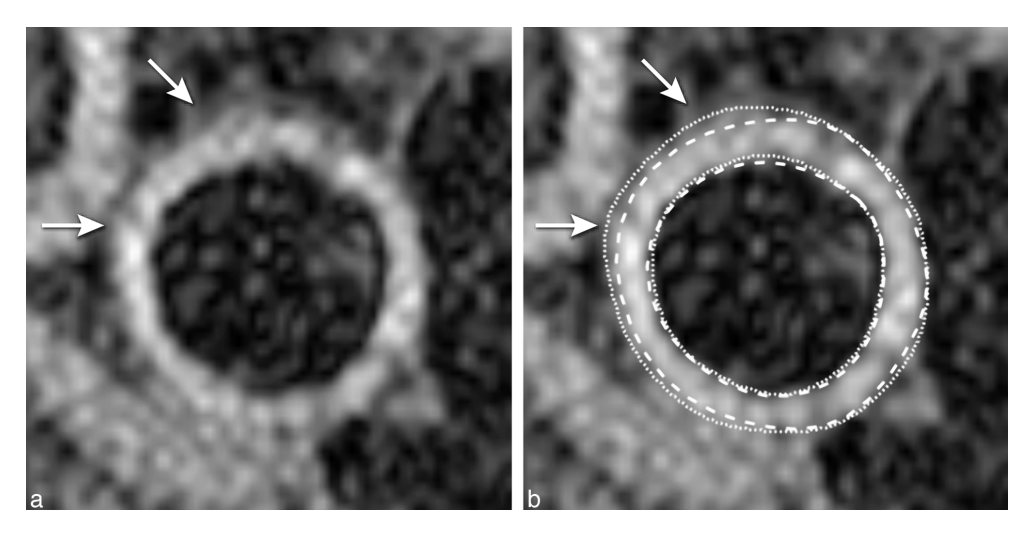


Figure 2.8: Example where the outer contour was fitted on the strongest edge, indicated by the arrows, but the manual contour was not drawn on the strongest edge (dotted = manual, striped = automatic).

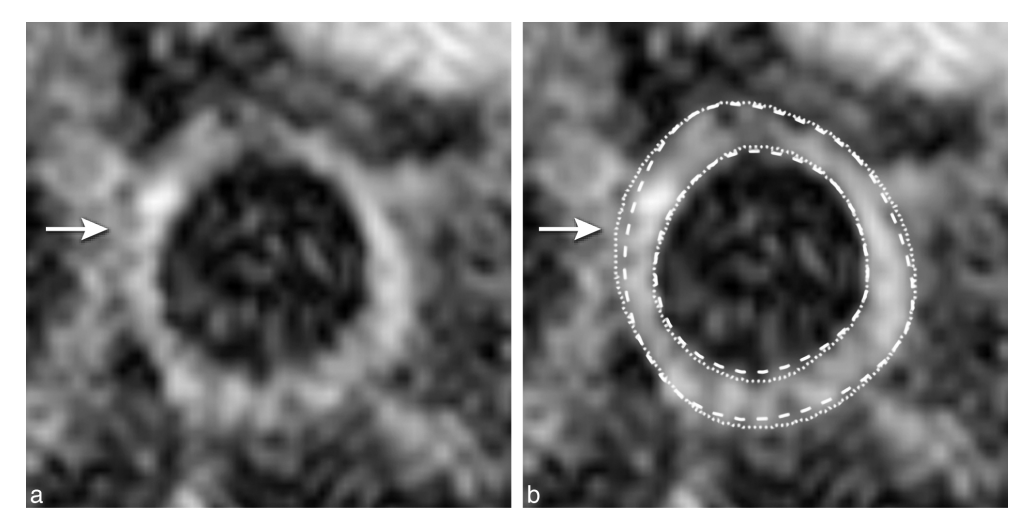


Figure 2.9: Example of weak edge information at the outer boundary (indicated by the arrow). The automatic contour is not attracted by an image edge, although the manual expert extrapolates the vessel in these areas (dotted = manual, striped = automatic).

of the automatically detected contours. The reported results, therefore, provide a realistic view on the practical applicability of the proposed analysis method.

Compared with other methods, our method requires minimal user interaction and has the advantage that it extracts 3D image information instead of acting independently on each vessel wall slice, which is the case for the existing segmentation methods.

Most of the disagreement in VWT and VWV was caused by small deviations in the segmentation of the outer wall. Small disagreements can be explained by the difference be-

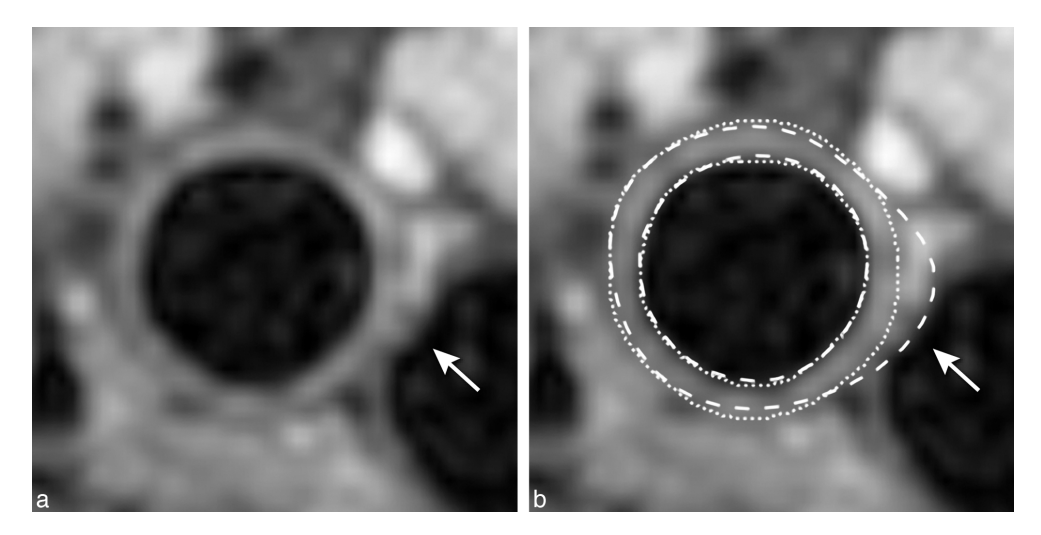


Figure 2.10: Incorrect segmentation of the outer vessel wall as indicated by the arrow. The outer tube is fitted to a strong edge which does not correspond to outer vessel wall (dotted = manual, striped = automatic).

tween the automatic and manual segmentation method. While the automatic method is designed to fit the tube surface on the strongest edge, a manual observer delineates the vessel wall based on its visual perception, which is subjective and also depends on the window/level setting of the display. This means that the observer does not necessarily draw on the strongest edge, an example can be seen in Figure 2.8; the strongest edge is not at the location of the outer boundary. The lumen boundary has a sharp edge in the image and is less sensitive to this effect. The outer boundary, especially for the more thickened vessels, is much more affected, explaining both the observed underestimation and proportional error in the quantification of the vessel wall dimensions.

Areas in the image with low image contrast are another source of errors. In those areas, an observer delineates the contours based on his experience and how it should look like, while the automatic segmentation either does not change its initial shape because there is no image force guiding the algorithm (Fig. 2.9), or the tube might be attracted by edges from nearby structures (Fig. 2.10). In our approach, image information from neighboring slices is taken into account to improve situations where edges are weak or missing.

This study is subject to several limitations. The presented automated method is dependent on the availability of a 3D MRA series. In this study, a Time of Flight MRA image is used to identify the artery of interest. In case this image is not available, the lumen center can also be detected directly in the vessel wall images. However, we did not investigate the impact on the performance when a MRA image is not present. Also the user interaction will become more complex because no global overview of the arterial structure is present and the artery of interest has to be indicated in the vessel wall slices.

In this study, the common carotid artery was analyzed. The 3D model can be adapted to support a bifurcating structure [59] including the internal carotid artery, however, obtaining good quality black blood vessel wall images in the carotid bifurcation is technically more challenging [60]. The shape of the carotid artery changes rapidly in the bifurcation and partial volume effect is very likely to appear when using a slice thickness of over 1

2.4. Discussion 27

mm. Isotropic 3D imaging of the bifurcation might overcome this problem.

The next step in the development and validation of this method is to address the observed underestimation and trend. The manual expert does not always draw the outer boundary on the maximum edge, especially in cases with higher VWT, but uses another criterion. A potential solution is to change the calculation of the image forces for the segmentation of the outer wall. Outer contours drawn by different manuals observers should be analyzed to get insight in the average SI profile of the outer boundary. Then the calculation of the image forces can be adapted by taking that average SI profile into account.

In conclusion, quantification of the vessel wall dimensions is an important tool in the research of atherosclerosis. Using automated segmentation reduces the processing time of the analysis and provides reproducible results. Even if manual corrections are needed in some images, the analysis time is still shorter than doing a complete manual segmentation. An additional advantage is the visualization of the 3D segmentation results. Different visualizations of the vessel wall can provide more insight in the condition of the artery because local shape and characteristics like asymmetry are more easily assessed. This study was performed with 2D vessel wall slices, but developments of MR pulse sequences are directed toward true 3D imaging [44,60–62]. In that case, manual segmentation of the image data becomes impractical due to the size of the dataset, while the presented method is already able to analyze isotropic image data.

Acknowledgments

This study was funded by the Dutch Technology Foundation STW, which is the applied science division of NWO, and the Technology Programme of the Ministry of Economic Affairs.